Synthesis and characterization of a dual-targeting, mitochondrial-immobilizing nanoparticle drug delivery system

THESIS

Presented in partial fulfillment of the requirements for Honors Research with Distinction in the Undergraduate School at The Ohio State University

By

Matthew William Becker

Undergraduate in Biomedical Engineering

The Ohio State University

2017

Thesis Committee:

Dr. Xiaoming He, Advisor

Dr. Katelyn Swindle-Reilly

Abstract

Cancer stem-like cells (CSCs) are rare subpopulations of cells that are drug resistant and have been shown to be responsible for the recurrence of cancer. CSCs are typically not responsive to traditional cancer treatments, so an alternative method, able to overcome the drug resistance of these subpopulations, is desirable. Nanoparticles are one potential solution to this problem and are currently under intense research. The aim of this study was to determine an ideal method (i.e. cheap, quick, and efficient) for synthesizing and loading nanoparticles with therapeutics for treating cancerous cells. A novel nanoprecipitation method was designed to create smaller and more homogeneous particles compared to the traditional nanoprecipitation method. We hypothesized that this method would be able to encapsulate therapeutic agents in Pluronic F127 and poly(L-lactic-co-glycolic acid) that would result in nanoparticles, further coated with triphenylphosphonium and hyaluronic acid for targeting capabilities, less than 200nm in diameter with surface charges below -20mV. Further, we hypothesized this method would result in higher encapsulation efficiencies of therapeutics and be able to target mitochondria *in vitro*. It was found that infusion rates of 20ml/hr for water and 4ml/hr for oil, a polymer concentration of 10mg/ml, and a 1:1 ratio of PLGA to PF127-TPP resulted in the smallest (168.48±6.3nm), most homogeneous nanoparticles (PDI = 0.05) with surface charges of -35.54±3mV. The encapsulation efficiency for porphyrin was 73.5±3.4%, but was lower for lonidamine and doxorubicin, at 36.3±5.2% and 21.9±15.1%, respectively. Mitochondrial targeting capabilities of the particles were confirmed with PLGA-PF127-TPP-Dox nanoparticles with MDA-MB-231 cells via confocal images and fluorescence overlap of doxorubicin with MitoTracker Deep Red dye. These results indicate that while more studies need to be done to determine drug release mechanisms and kinetics and targeting capabilities of PLGA-PF127-TPP-HA nanoparticles, the novel method described here is viable for creating dual targeting nanoparticles capable of treating drug resistant phenotypes of CSCs.

Acknowledgements

The author would like to thank Associate Professor Dr. Xiaoming He for his advising on this project, post-doctoral researcher Dr. Jiangsheng Xu for his project collaboration and helpfulness, and the Ohio State Undergraduate Research Office in the College of Engineering for their support towards the research proposal.

Table of Contents

List of Figures

Chapter 1: Introduction

1.1 Background

Within the field of cancer, cancer stem-like cells (CSCs) have attracted much attention in recent years. CSCs are capable of self-renewal to maintain stemness, as well as differentiating into all types of residual cells associated with the original tumor. Additionally, a drug resistant phenotype tends to arise across most CSC populations. These phenotypes arise either due to an overexpression of drug efflux pumps in the cell or maintenance of a somewhat dormant state in which the cells metabolize substances much slower than the surrounding tumor. As such, evidence has shown that these types of cells are partially responsible for tumor recurrence[1,2,3].

A method for treating cancer that has seen huge strides since its inception is the use of therapeutic nanoparticles. There are several advantages to using nanoparticles as opposed to traditional chemotherapy. First, nanoparticles have small, tunable sizes. The rapid growth of tumors causes them to have a leaky vasculature compared to normal tissue, and this gives rise to what is known as the enhanced permeability and retention (EPR) effect. Pores in tumor vasculature are larger than they are for normal tissue, ranging from ~20-250nm. Nanoparticles in this size range can leak into tumor tissue but not normal tissue, thus taking advantage of the EPR effect. Another benefit to using nanoparticles is that they can encapsulate and deliver a wide variety of therapeutic agents. Not only can they encapsulate normal therapeutic drugs for effective *in vivo* delivery[4], but they can also encapsulate combinations of drugs and RNA to reverse drug resistance in cancer cells[5]. Finally, nanoparticles can be modified to target cancer cells beyond the EPR effect. By modifying the surfaces of nanoparticles with ligands for cell surface receptors that are overexpressed in the cancer cell line of interest, they effectively become highly targeted and more efficient at delivering their payloads to the intended cells[4,6]. A

common modification is the addition of hyaluronic acid (HA) onto the surface of nanoparticles. This is because HA is a ligand for the CD44 cell surface receptor that is overexpressed in many types of cancers and CSCs, and has been shown to be effective at targeting tumors *in vivo*[7].

Besides being able to target at the cellular level, nanoparticles can also target at the organelle level. One molecule of interest here was triphenyphosphonium (TPP), which is capable of targeting and binding to mitochondria. TPP is a lipophilic cation that takes advantage of the strong negative membrane potential of mitochondria to bind and internalize in the mitochondrial matrix. Marrache et al. have shown that nanoparticles modified with TPP on their surfaces are capable of targeting mitochondria *in vitro*[8]. Mitochondria have become attractive targets for anti-cancer drugs. The reasons for this are two-fold: first, mitochondria are crucial for cell survival as they are responsible for most of the ATP production within cells and thus provide most of the energy needed for cellular processes; second, it has been found that mitochondria are crucial regulators of apoptotic pathways due to their regulation of the translocation of pro-apoptotic proteins from the mitochondrial intermembrane space to the cytosol[9]. One of the most prolific phenotypes across all cancer cell lines is characterized by suppressed apoptotic pathways, therefore mitochondria-directed delivery of drugs that are designed to trigger apoptosis would provide a promising strategy for treating cancer.

One of the most common methods used to synthesize nanoparticles is nanoprecipitation. In this method, an organic phase consisting of the desired polymers and drugs – dissolved in organic solvents – is added dropwise to de-ionized water while stirring. Three important aspects here are that the organic solvents be mostly immiscible in water, the polymers used are amphiphilic, and the intended payloads are hydrophobic. If these conditions are met, then when the organic phase is added to the water phase, the polymer blocks will self assemble and trap the

payload in their core. The organic solvents are then evaporated out, and the nanoparticle solutions can be washed and collected. To achieve nanoparticles with higher encapsulation efficiencies, slower drug release, and lower polydispersity, several groups of researchers have used microfluidics approaches with co-axial, focused streams in either a 2D[10] or 3D manner[11].

1.2 Motivation

The motivation for this study arises from a few areas. First, as mentioned before, CSCs are often unaffected by traditional chemotherapies and are linked to the recurrence of tumors. Thus, it is desirable to find a method that is capable of eradicating CSC populations along with the rest of the tumor. One method that has shown promise in this area is mitochondrial targeting of cancer cells. Nanoparticles that are coated with mitochondrial targeting moieties are particularly effective at delivering their payloads to cancer cells and have the potential to overcome any drug resistant phenotypes that may be present in the cancer cell populations being treated, including CSCs. Finally, while nanoprecipitation methods are viable for synthesizing nanoparticles, there is room for improvement in several areas. Microfluidics approaches attempt to solve these problems, but they may get overly complicated or expensive. Finding a cheap, easy to set up and use alternative to microfluidics nanoprecipitation that still retains the benefits would be an important step in nanoparticle research.

1.3 Significance

The significance of this study relates directly to cancer and its burden on humans. According to the World Health Organization, cancer is the second leading cause of death globally and was responsible for 8.8 million deaths in 2015. Just in the United States alone, an estimated 1.7 million new cases of cancer were diagnosed in 2017[12]. Not only is there a burden on human life, but cancer is also a large economic strain. National expenditures for cancer care totaled nearly $125 billion in 2010[11]. From these statistics, it is evident that cancer will continue

to be a problem both economically and in terms of human death, unless cheaper, more effective methods of treatment that mitigate the chances for relapse are pursued.

1.4 Specific Aims

Aim 1: Prepare a biodegradable and biocompatible, multifunctional, nanoscale drug delivery system via a novel nanoprecipitation method capable of selectively targeting mitochondria. *We hypothesize that using a novel nanoprecipitation method to encapsulate therapeutic agents in Pluronic F127 and poly(L-lactic-co-glycolic acid) will result in nanoparticles, further coated with triphenylphosphonium and hyaluronic acid, less than 200nm in diameter with surface charges below -20mV.*

Aim 2: Evaluate the drug encapsulation efficiency and mitochondrial immobilizing capabilities of the drug delivery system *in vitro. We hypothesize that this method will result in higher encapsulation efficiencies compared to traditional nanoprecipitation and particles and their payloads will be able to selectively target mitochondria.*

Chapter 2: Methods

2.1 Preparation of compounds

Prior to any nanoparticle synthesis, several compounds had to be prepared. The chemical synthesis and modification techniques used were outside the scope of this study, but are worth noting to avoid confusion. Please direct all inquiries in the matter to Dr. Jianghsheng Xu, postdoctoral researcher in Dr. He's lab. The encapsulated drug that was used for most of this study was a derivative of porphyrin, modified to have a benzyl chloride group (Ps-Cl), which was previously shown to be mitochondrial targeting[13]. TPP was also synthesized prior to the start of this study. Additionally, Pluronic F127 (PF127) modified with TPP (PF127-TPP) had to be prepared prior to nanoparticle synthesis.

2.2 Nanoparticle synthesis

Nanoparticles were synthesized using a somewhat novel nanoprecipitation method (**Error! Reference source not found.**). A double lumen needle, typically used for electrospinning, was used to create co-axial streams of the two liquid phases. Inlet 1 was the organic phase and the inner stream while Inlet 2 was the water phase and outer stream. Since this was a somewhat novel method, we wanted to explore various conditions to find optimal ones.

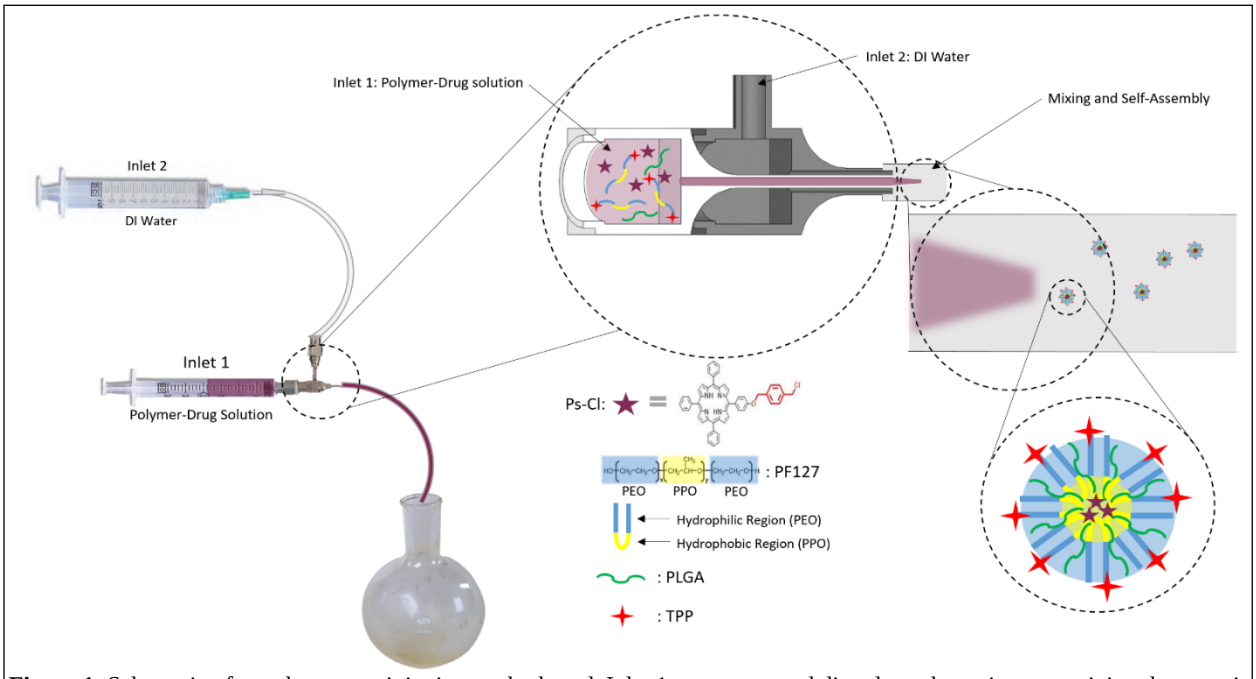

Figure 1: Schematic of novel nanoprecipitation method used. Inlet 1 was connected directly to the syringe containing the organic phase, while Inlet 2 was connected via Tygon tubing to the syringe containing water. Tygon tubing was also used to connect the needle to the flask. It was made sure that the end of the tube was underneath the surface of the fluid in the flask. Upon reaching the outlet of the needle, the two phases underwent mixing, and the amphiphilic polymers self assembled trapping the hydrophobic Ps-Cl in their core.

Initially, different concentrations of PF127 (without TPP modification) were dissolved in the oil phase. For each condition, the concentration of Ps-Cl was kept the same at 2mg/ml and the total volume of the organic phase was kept the same at 2ml. Ps-Cl was dissolved in tetrahydrofuran (THF) and PF127 was dissolved in acetonitrile (ACN). To have 2ml of the organic phase (sometimes referred to as oil), 2mg of Ps-Cl was dissolved in 1ml THF and added

to either 20, 40, or 100mg PF127 dissolved in 1ml ACN (for 10, 20, or 50mg/ml, respectively). This way, the drug to oil ratio was kept the same throughout each condition. De-ionized (DI) water was used and kept at a ratio of 10:1 (v:v) to oil. The total volume of water was split equally between a syringe and a round bottom flask, with 10ml in each. Using syringe pumps, water was infused into the flask at a rate of 10ml/hr and the organic phase was infused at a rate of 2ml/hr. Since Ps-Cl is light sensitive, the nanoparticle synthesis process was protected from light as much as possible. After both phases had been completely infused, the mixture was allowed to stir for an additional hour. Following this, the solution was centrifuged at 13600 G for 10 minutes to collect the nanoparticles and the supernatant was removed. Nanoparticles were washed with DI water twice before final collection. Higher infusion rates were also tested with all three concentrations of PF127. They were 20ml/hr and 4ml/hr for the water and oil phases, respectively.

Once it had been determined what polymer concentrations and infusion rates resulted in the smallest and most homogeneous nanoparticle populations, poly(L,lactic-co-glycolic acid) (PLGA) was added to the organic phase. At this point, we also began using PF127-TPP. The ratio of PLGA to PF127-TPP was varied to find optimal conditions. The conditions tested were 1:1, 1:3, and 1:1.5 (PLGA:PF127-TPP). Both polymers were dissolved together in ACN. Again, the water to oil ratio was kept constant at 10:1 (v:v), and the Ps-Cl concentration was kept constant at 2mg/ml. Total volumes used were 20ml DI water (10ml in the syringe and 10ml in the flask) and 2ml organic phase. Using the optimal polymer concentration and infusion rates, nanoparticles were synthesized and allowed to mix for an additional hour after infusion had ceased. The same process for nanoparticle collection that was outlined above was used here as well.

2.3 Hyaluronic acid modification

After nanoparticles had been synthesized with PLGA, PF127-TPP, and PS-Cl (PPP-T), they were further modified with HA. Briefly, 1mg of PPP-T nanoparticles were dispersed in 5ml DI water. Additionally, 3mg HA was dissolved in 1ml DI water. The nanoparticle solution was put under magnetic stirring and the HA solution was added dropwise. After HA addition, the mixture was allowed to mix for 4 hours under a closed atmosphere. The entire solution was centrifuged at 13600 G for 10 minutes, the supernatant was poured off, and the particles were washed with DI water before final collection.

2.4 Nanoparticle characterization

Nanoparticle size and surface potential were analyzed using a Brookhaven (Holtsville, NY) 90 Plus/BI-MAS dynamic light scattering (DLS) instrument by dispersing nanoparticles (500µg/ml) in DI water. Nanoparticle size and morphology was also characterized using transmission electron microscopy (TEM). Nanoparticles were examined after being negatively stained with uranyl acetate solution (2% w/w) using an FEI (Moorestown, NJ) Tecnai G2 Spirit transmission electron microscope.

2.5 Drug encapsulation efficiency

Once the optimal conditions for nanoparticle synthesis had been determined (i.e. which conditions resulted in the smallest, most homogeneous particles), the encapsulation efficiency of Ps-Cl was analyzed. The amount of Ps-Cl encapsulated was determined spectrophotometrically using a Beckman Coulter (Indianapolis, IN) DU 800 UV-Vis spectrophotometer based on its absorbance at 405mn. The amount of Ps-Cl not encapsulated (free Ps-Cl) was determined by taking 200µl of the supernatant liquid after centrifuging a nanoparticle solution and adding it to 2ml of DI water. The absorbance of this was compared to 200µl of the nanoparticle solution before centrifugation in 2ml DI water (PPP-T NPs + free Ps-Cl). Empty nanoparticles were also

made and their absorbance was measured to determine the contribution of particles to the PPP-T NPs + free Ps-Cl solution. The encapsulation efficiency was calculated using the following equation:

$$EE = \frac{A_{PPP-T} - A_{Empty}}{A_{PPP-T} - A_{Empty} + A_{Ps-Cl}}$$

where $A_{PPP\text{-}T}$ is the absorbance of PPP-T nanoparticles and un-encapsulated Ps-Cl, A_{Empty} is the absorbance of empty PLGA-PF127-TPP nanoparticles, and $A_{Ps\text{-}Cl}$ is the absorbance of free Ps-Cl. All absorbance values were taken at 405nm.

2.6 Encapsulating different drugs

In addition to encapsulating Ps-Cl using this nanoprecipitation method, we also wanted to show that it would be viable for other, less hydrophobic drugs. To test this, we used two common cancer drugs, lonidamine (Lon) and doxorubicin (Dox). Nanoparticles were synthesized using the previously determined optimal conditions, except with 2mg/ml Lon (PPL-T) or Dox (PPD-T) instead of Ps-Cl. Lonidamine was dissolved in THF. The stock Dox product available was a hydrochloride salt, making it soluble in water and not ideal for nanoprecipitation. Thus, we dissolved Dox in 2ml methanol and added 5µl triethylamine (TEA) to obtain free Dox, which is more hydrophobic. Barring this exception, the same protocol outlined above was used for synthesis, collection, characterization, and determination of encapsulation efficiency for these nanoparticles. Nanoparticles encapsulating Lon and Dox did not undergo HA modification at any point.

2.7 Determination of mitochondrial targeting

PPD-T nanoparticles were used to determine the mitochondrial targeting capabilities of nanoparticles with TPP modification *in vitro*. MDA-MB-231 human breast cancer cells (ATCC, Manassas, VA) were cultured in DMEM supplemented with 10% FBS and 1% Pen Strep at 37°C

in a humidified 5% CO_2 incubator. Media was changed every other day. Once cells had reached at least 70% confluency, they were passaged and seeded into individual 35mm dishes with cover glasses at $2x10^5$ cells/dish and incubated for an additional 24 hours. Then, the media was replaced with 2ml of either free Dox at 5µg/ml DMEM, PPD nanoparticles at 60µg/ml DMEM, or PPD-T nanoparticles at 60µg/ml DMEM. After incubation for 4 hours, that media was removed and cells were stained with DAPI and MitoTracker Deep Red FM dyes and then fixed. Cover glasses were mounted onto glass slides with anti-fade mounting medium (Vector Laboratories Burlingame, CA) for examination using an Olympus FluoView™ FV1000 confocal microscope.

Chapter 3: Results and Discussion

3.1 Determination of optimal conditions

As seen in Figure 2a, the optimal conditions in regards to polymer concentration and infusion rates as determined by DLS were 10mg/ml for the polymer concentration, 20ml/hr for the water infusion rate, and 4ml/hr for the oil infusion rate. These conditions created nanoparticles that were 50.49±11.9nm in diameter, with a polydispersity (PDI) of 0.225. Using a smaller polymer concentration and faster infusion rates ultimately allowed for less contact time between less materials. The fact that there were less materials in the organic phase and less time for them to be in contact with each other in a uniform fashion (before being expelled from the tube into the flask) can account for the smaller, more homogeneous nanoparticles that resulted.

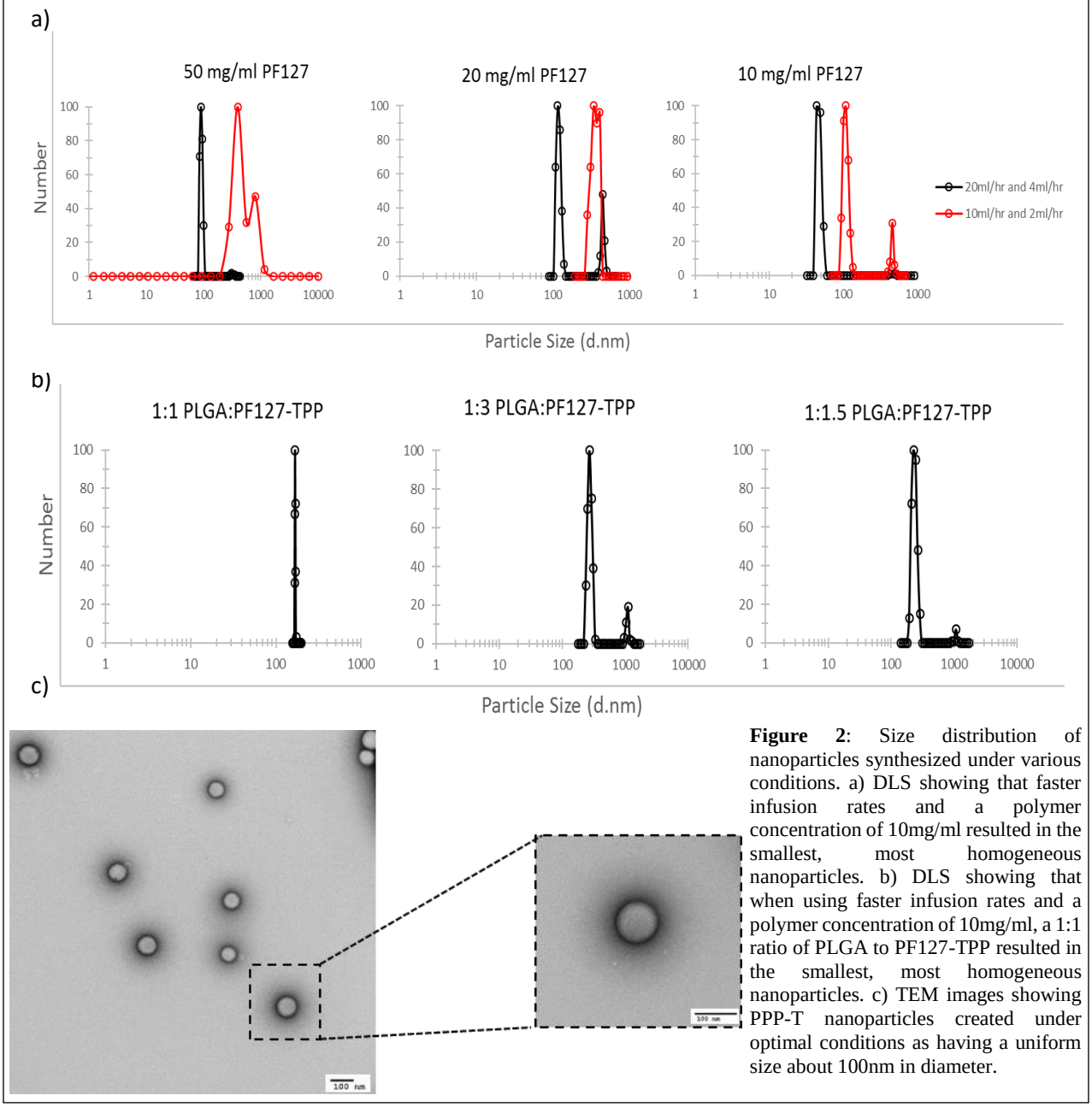

Figure 2: Size distribution of nanoparticles synthesized under various conditions. a) DLS showing that faster infusion rates and a polymer concentration of 10mg/ml resulted in the smallest, most homogeneous nanoparticles. b) DLS showing that when using faster infusion rates and a polymer concentration of 10mg/ml, a 1:1 ratio of PLGA to PF127-TPP resulted in the smallest, most homogeneous nanoparticles. c) TEM images showing PPP-T nanoparticles created under optimal conditions as having a uniform size about 100nm in diameter.

There was less of a chance for the amphiphilic polymer molecules to interact with each other – and less polymer molecules to interact overall – to form larger aggregates. Thus, only small nanoparticles, all approximately the same size, resulted from a polymer concentration of 10mg/ml and infusion rates of 20ml/hr for water and 4ml/hr for oil.

Additionally, it was found that using a PLGA to PF127-TPP ratio of 1:1 was ideal (Figure 2b). Using all of these conditions together created by far the most homogeneous

population of nanoparticles that was seen in this study with a polydispersity of 0.05. PLGA is much more hydrophobic than just PF127, which would account for the extremely low PDI. Figure 2c shows a TEM image of PPP-T nanoparticles having a very uniform size distribution. Although TEM images showed these nanoparticles to be about 100nm in size, DLS measurements gave a value of 168.48±6.3nm. This difference between TEM and DLS is typical, as the value given from DLS can be heavily swayed by only a few larger particles, skewing the result to a larger value. PPP-T nanoparticles were larger than those with just PF127, but that is likely due to the addition of TPP and PLGA.

Varying the ratio of PLGA to PF127-TPP while keeping the overall polymer concentration constant at 10mg/ml required using less PLGA for the 1:3 and 1:1.5 ratios (5mg and 8mg, respectively), as opposed to using 10mg for the 1:1 ratio. Reducing the amount of PLGA from 10 to 8mg, and from 8 to 5mg, resulted in larger and less homogeneous nanoparticles each time (260.50±5.0nm with PDI 0.219 and 360.90±13nm with PDI 0.278 for 1:1.5 and 1:3, respectively). Including less of the very hydrophobic PLGA in the organic phase meant that the overall hydrophobicity of that phase was decreased, which gave rise to larger, less homogeneous nanoparticles.

3.2 Hyaluronic acid modification

Hyaluronic acid modification was confirmed via zeta potential measurements taken with DLS (Figure 3). Plain PF127 nanoparticles have a negative surface charge (-48.17±2.16mV), but once PF127 had been modified with TPP, nanoparticles had a positive surface charge (38.21±7.57mV). This shift from negative to positive surface charges makes sense, as TPP is a highly cationic molecule. HA on the other hand, is anionic. As such, modification of HA onto PPP-T nanoparticles took place via simple electrostatic interactions between TPP and HA. The resulting surface charge of nanoparticles (PPP-TH) was thus negative once again (-35.54±3mV).

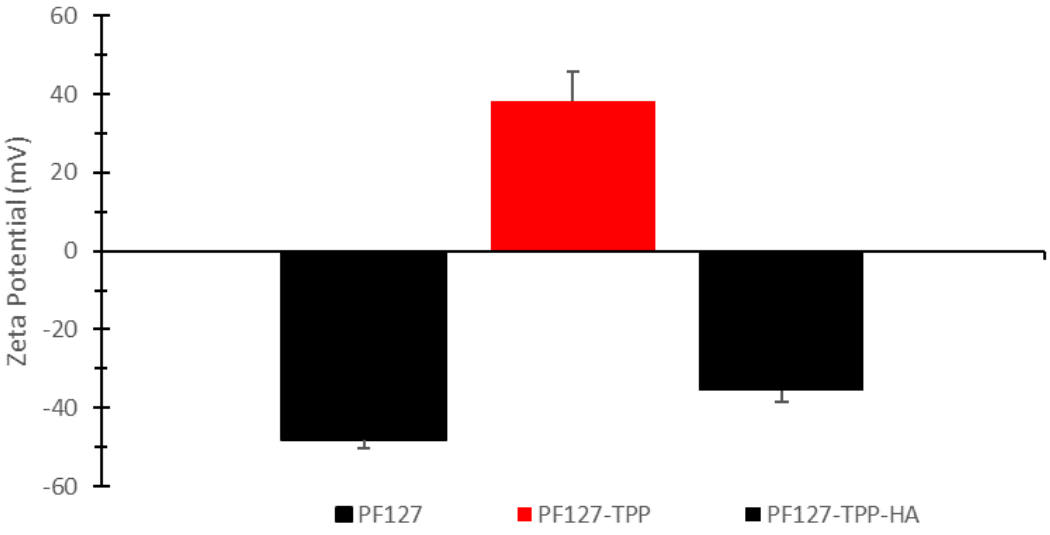

Figure 3: Surface charges of nanoparticles at various stages of modification. TPP modification caused the surface charge of PF127 nanoparticles to become positive, while HA modification was confirmed via a negative surface charge.

Modification with HA is in theory important in more than just cellular targeting via CD44 receptors. The electrostatic interactions between HA and TPP are stable at a normal body pH (~7.4). However, the pH in tumor microenvironments is more acidic than normal (~6.0) mostly due to hypoxic conditions. Further, the pH of cell transport vesicles such as endosomes and lysosomes is even lower (~5.0). As the pH of the solution that PPP-TH nanoparticles are in decreases, it is thought that the electrostatic interactions between TPP and HA are disrupted. Eventually TPP and HA will dissociate, and we think that this dissociation will disrupt the stability of the entire nanoparticle, resulting in release of the payload inside the cell.

3.3 Encapsulation efficiency of Ps-Cl

First, to confirm that PPP-T nanoparticles were encapsulating Ps-Cl, the absorbance of loaded PPP-T nanoparticles was compared to free Ps-Cl at 405nm. Both samples had the same peak, confirming encapsulation. With this confirmed, the encapsulation efficiency of Ps-Cl within PPP-T nanoparticles was investigated and found to be 73.5±3.4%. This is higher than values that were found for typical nanoprecipitation methods, which tend to fall within 45-65%

encapsulation. This could be for a number of reasons. First, Ps-Cl is an exceptionally hydrophobic drug, which automatically makes it an ideal candidate for nanoprecipitation methods. Second, this method provides a much more uniform process for nanoparticle formation than traditional nanoprecipitation. The co-axial streams allow for homogeneous mixing between the water and oil phases before they even reach the flask, whereas in traditional methods the oil phase is added directly into the flask and mixed under turbulent, heterogeneous conditions. Either of these could account for the high encapsulation efficiency of Ps-Cl. While a direct comparison was not made between encapsulation efficiencies using the method described here and a traditional nanoprecipitation method, we still believe that the novel method would result in higher encapsulation of Ps-Cl.

3.4 Encapsulating Lonidamine and Doxorubicin

Nanoparticles encapsulating Lon and Dox formed using this novel method did not see as promising results as those encapsulating Ps-Cl (Figure 4). PPL-T nanoparticles had a mean diameter of 253.51±19.0nm and a PDI of 0.434. Further, the encapsulation efficiency of Lon was only 36.3±5.2%. Oddly, the surface charge of PPL-T nanoparticles was measured to be -41.63 ±2.1mV. The high PDI and low encapsulation efficiency could be due to Lon being somewhat hydrophilic. Its more hydrophilic nature would allow for more interactions with water and thus less of a chance of being encapsulated. Additionally, if it was encapsulated it might bring water molecules along with it into the core of nanoparticles, effecting their size and homogeneity. The negative surface charge of PPL-T nanoparticles is harder to explain. It may also have something to do with the hydrophilicity of Lon and the subsequent lack of homogeneity, but we are ultimately unsure as to why this was observed.

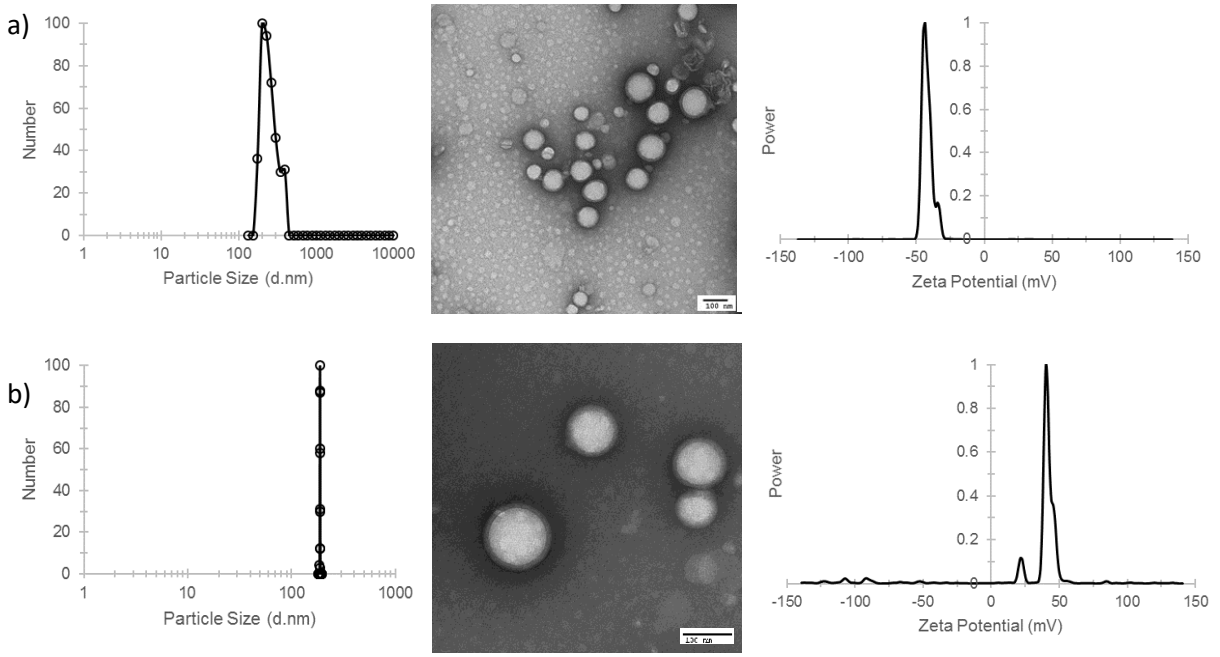

Figure 4: Size and surface charge of PPL-T and PPD-T nanoparticles. a) DLS and TEM both show larger PPL-T nanoparticles with a less homogeneous size distribution than PPP-T. Oddly, the surface charge of PPL-T particles was strongly negative. b) PPD-T nanoparticles were very homogeneous in both DLS and TEM measurements, although slightly larger than PPP-T nanoparticles. Surface charge of PPD-T particles was positive as expected, but not as homogeneous as PPP-T.

While the PDI of PPD-T nanoparticles was very low (0.003), the mean diameter was slightly larger than PPP-T nanoparticles at 188.66±3.0nm. The encapsulation of Dox was much lower than Ps-Cl at 21.9±15.1%. The surface charge of PPD-T particles was positive as expected at 41.12±21.8mV, although less homogeneous than PPL-T nanoparticles, as is indicated by the high standard deviation and secondary peak at 23mV. While free Dox is a hydrophobic drug, the method used to obtain free Dox may have been inefficient and thus affected the encapsulation efficiency and zeta potential. As stated in the methods section, the stock Dox powder was a hydrochloride salt, making it soluble in water. To rid the Dox of the hydrochloride group, it was dissolved in methanol and TEA. This freeing method may not have been totally efficient, leaving some hydrophilic Dox in solution. In addition, methanol is fairly miscible in water. Nanoprecipitation methods take advantage of the hydrophobic and immiscible nature of the

organic phase, so having hydrophilic Dox and a miscible organic phase could have effected subsequent nanoparticle formation and encapsulation.

3.5 Mitochondrial targeting

While it would have been ideal to confirm the mitochondrial targeting of both TPP modified nanoparticles and Ps-Cl, it was only possible to determine the former. Ps-Cl is an inherently photoluminescent molecule with an emission peak around 650nm. At the time of this study, there was no confocal microscopes available with that particular wavelength of light, so Ps-Cl could not be detected. Instead, we used PPD-T nanoparticles and took advantage of the photoluminescent properties of Dox to test mitochondrial targeting of TPP modified nanoparticles *in vitro* (Figure 5).

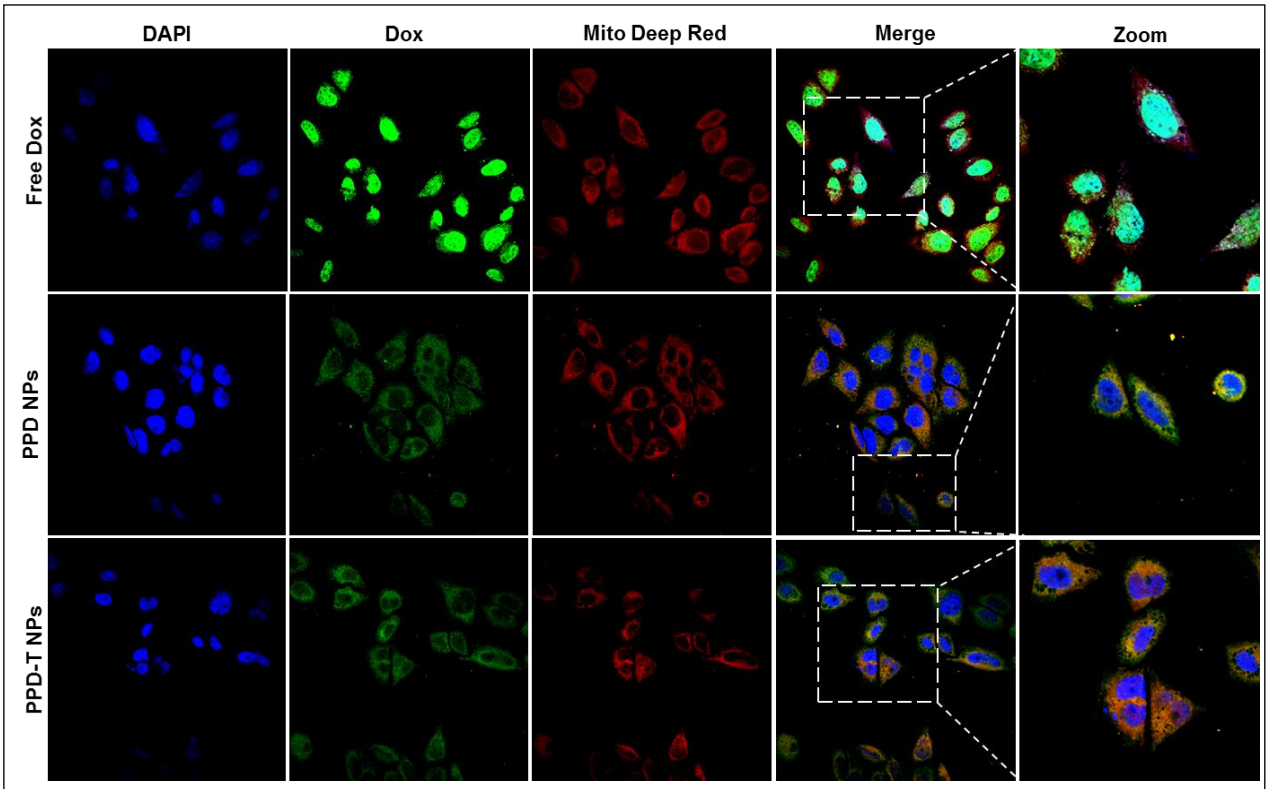

Figure 5: Confocal images showing mitochondrial targeting of TPP modified nanoparticles. An orange color seen in the merge indicates an overlap of Dox and Mito Deep Red, confirming targeting. This color is more prevalent in the PPD-T group than the PPD and Free Dox groups.

After incubating 231 cells with either free Dox, PPD (untargeted) nanoparticles, or PPD-T (targeted) nanoparticles for 4 hours, confocal images confirmed the targeting capabilities of TPP modified nanoparticles *in vitro*. Free Dox – once in cells – gathers in the nucleus, so it was expected to see an overlap of free Dox and DAPI, but not with Mito Deep Red. Dox encapsulated in nanoparticles however, would most likely not be able to get in the cell nuclei thus remaining in the cytosol. Cells treated with untargeted PPD nanoparticles did show Dox in the cytosol and not the nuclei, but there was not a good overlap with mitochondria. Rather, there appeared to be individual red and green areas in the overlap with only minimal orange areas. However, cells treated with targeted PPD-T nanoparticles showed an excellent overlap between Dox and mitochondria, as was indicated by the orange color seen in most cells in the overlapped images. The fluorescent intensity of Dox also appears to be stronger in cells treated with PPD-T particles than PPD particles. The addition of highly cationic TPP to nanoparticles and overall positive surface charge makes cellular uptake much easier, which accounts for this observation. Thus, while confirming mitochondrial targeting of both Ps-Cl and TPP would have been desirable, it was at least confirmed for TPP modified nanoparticles.

Chapter 5: Conclusions

In this study, we aimed to create small, homogeneous nanoparticles capable of encapsulating therapeutic drugs using a somewhat novel nanoprecipitation method. Additionally, we sought to modify the surfaces of these nanoparticles with TPP, a mitochondrial targeting moiety, and HA, a ligand for the CD44 cell surface receptor overexpressed in many types of cancers. We found that with this double lumen needle method, a polymer concentration of 10mg/ml, infusion rates of 20ml/hr for water and 4ml/hr for oil, and a 1:1 ratio of PLGA to PF127-TPP created the smallest, most homogeneous nanoparticles. Nanoparticles encapsulating

Ps-Cl using this method were 168.48±6.3nm with a PDI of 0.05. The encapsulation efficiency of Ps-Cl was also high, at 73.5±3.4%. While a direct comparison was not made between this method and a traditional nanoprecipitation method, these results still indicate that the method described here may be superior to others. Using a double lumen needle for nanoprecipitation can result in nanoparticle homogeneity and encapsulation efficiencies similar to those seen in microfluidics studies. However, this method is not as complicated, time consuming, or expensive as microfluidics approaches, giving it an advantage.

Successful modification with both TPP and HA was confirmed via zeta potential measurements. The addition of TPP resulted in an overall positive surface charge of 38.21±7.57mV for nanoparticles, while HA addition resulted in an overall negative surface charge of -35.54±3.0mV. The use of mitochondrial targeting agents (i.e. TPP and Ps-Cl) gives this nanoparticle platform the potential to treat drug resistant populations of both typical cancer cells and CSCs. Further, the addition of HA to nanoparticles gives them the ability to target cancer cells that overexpress the CD44 cell surface receptor, which is a common phenotype. The electrostatic interactions between TPP and HA may also be a potential mechanism for drug release once the nanoparticles are internalized in cells. Despite this phenomenon not being directly examined in this study, it would be straightforward to analyze in future experiments.

Within this study, only the targeting capabilities of TPP modified particles without HA were examined. Using PPD-T nanoparticles that had a lower encapsulation efficiency than PPP-T particles, TPP targeting was confirmed via confocal microscopy images. Future studies would seek to measure the targeting capabilities of Ps-Cl and HA modified nanoparticles in both 2D and 3D cultures *in vitro*. We would also seek to improve the encapsulation efficiencies of Lon, Dox, and possibly other drugs, as well as consider this method for being able to encapsulate

multiple therapeutic agents at a time. Additionally, we would want to test the efficacy of PPP-TH nanoparticles in a stem cell enriched 3D environment *in vitro* in killing malignant cell populations. After this, *in vivo* studies might be conducted with PPP-TH nanoparticles to examine how effective they are in a true biological system and how they are metabolized within the body. Despite the limitations and drawbacks of this study, it was able to show that this method is viable for synthesizing nanoparticles capable of targeting drug resistant cells and CSC sub-populations, and it an important step in treating cancer in a cheap, efficient, and complete manner.

References

1. Liu, Can, K. Kelnar, B. Liu, X. Chen, T. Calhoun-Davis, H. Li, L, Patrawala, H. Yan, C. Jeter, S. Honorio, J.F. Wiggins, A.G. Bader, R. Fagin, D. Brown, and D.G. Tang. "The microRNA miR-34a inhibits prostate cancer stem cells and metastasis by directly repressing CD44." *Nature Medicine* 17.2 (2011): 211-216.
2. Jordan, Craig T., M.L. Guzman, and M. Noble. "Cancer Stem Cells." *The New England Journal of Medicine* 355.12 (2006): 1253-1261.
3. Patrawala, L, T. Calhoun, R. Schneider-Broussard, H. Li, B. Bhatia, S. Tang, J.G. Reilly, D. Chanrda, J. Zhou, K. Coghlan, and D.G. Tang. "Highly purified CD44+ prostate cancer cells from xenograft human tumors are enriched in tumorigenic and metastatic progenitor cells." *Oncogene* 25.12 (2006): 1696-1708.
4. Fasehee, Hamidreza, R. Dinarvand, A. Ghavamzadeg, M. Esfandyari-Manesh, H. Moradian, S. Faghihi, and S.H. Ghaffari. "Delivery of disulfiram into breast cancer cells using folate-receptor-targeted PLGA-PEG nanoparticles: *in vitro* and *in vivo* investigations." *J. of Nanobiotech* 14.32 (2016).
5. Yi, Huqiang, L. Liu, N. Sheng, P. Li, H. Pan, L. Cai, and Y. Ma. "Synergistic therapy of doxorubicin and miR-129-5p with self-crosslinked bioreducible polypeptide nanoparticles reverses multidrug resistance is cancer cells." *Biomacromolecules* 17.5 (2016): 1737-1747.
6. Wang, Hai, P. Agarwal, S. Zhao, R.X. Xu, J. Yu, X. Lu, and X. He. "Hyaluronic acid-decorated dual responsive nanoparticles of Pluronic F127, PLGA, and chitosan for targeted co-delivery of doxorubicin and irinotecan to eliminate cancer stem-like cells." *Biomaterials* 72 (2015): 74-89.
7. Auzenne, Edmond, S.C. Ghosh, M. Khodadadian, B. Rivera, D. Farquhar, R.E. Price, M. Ravoori, V. Kundra, R.S. Freedman, and J. Klostergaard. "Hyaluronic Acid-Paclitaxel: Antitumor Efficacy against CD44(+) Human Ovarian Carcinoma Xenografts." Neoplasia 9.6 (2007): 479-486.
8. Marrache, Sean, R.K. Pathak, and S. Dhar. "Formulation and optimization of mitochondria-targeted polymeric nanoparticles." *Mito Med Vol II, Manipulating Mito Func.* 1265 (2015): 103-112.
9. Fulda, Simone, L. Galluzzi, and G. Kroemer. "Targeting mitochondria for cancer therapy." *Nature Reviews Drug Discovery* 9 (2010): 447-464.
10. Karnik, Rohit, F. Gu, P. Basto, C. Cannizzaro, L. Dean, W. Kyei-Manu, R. Langer, and O.C. Farokhzad. "Microfluidic platform for controlled synthesis of polymeric nanoparticles." *Nano letters* 8.9 (2008): 2906-12.
11. Rhee, Minsoung, P.M. Valencia, M.I. Rodriguez, R. Langer, O.C. Farokhzad, and R. Karnik. "Synthesis of size-tunable polymeric nanoparticles enabled by 3D hydrodynamic flow focusing in single-layer microchannels." *Adv. Mater* 23.12 (2011): H79-83.
12. "Cancer Statistics." *National Cancer Institute*. N.N., 22 Mar. 2017. Web <https://www.cancer.gov/about-cancer/understanding/statistics>.
13. Xu, Jiangsheng, F. Zeng, H. Wu, C. Hu, and S. Wu. "Enhanced photodynamic efficiency achieved via a dual-targeted strategy based on photosensitizer/micelle structure." *Biomacromolecules* 15 (2014): 4249-49.